Concentrating Membrane Proteins Using Asymmetric Traps and AC Electric Fields

12 AUTHORS, INCLUDING:

Jonathan Peter Bramble
University of Nottingham
50 PUBLICATIONS **279** CITATIONS

SEE PROFILE

Lukasz Krzeminski
Cornell University
11 PUBLICATIONS **179** CITATIONS

SEE PROFILE

Julea N Butt
University of East Anglia
126 PUBLICATIONS **2,674** CITATIONS

SEE PROFILE

Stephen D Evans
University of Leeds
227 PUBLICATIONS **6,200** CITATIONS

SEE PROFILE

Concentrating Membrane Proteins Using Asymmetric Traps and AC Electric Fields

Matthew R. Cheetham,[†] Jonathan P. Bramble,[†] Duncan G. G. McMillan,[†,‡,§] Lukasz Krzeminski,[†,§] Xiaojun Han,[†] Benjamin R. G. Johnson,[†] Richard J. Bushby,[§] Peter D. Olmsted,[†] Lars J. C. Jeuken,[†,‡,§] Sophie J. Marritt,[⊥] Julea N. Butt,[⊥] and Stephen D. Evans*,[†]

[†]School of Physics & Astronomy, University of Leeds, Woodhouse Lane, Leeds LS2 9JT, U.K.

[‡]Institute of Membrane and Systems Biology, University of Leeds, Leeds LS2 9JT, U.K.

[§]Centre for Molecular Nanoscience, University of Leeds, Woodhouse Lane, Leeds LS2 9JT, U.K.

[⊥]School of Chemistry, University of East Anglia, Norwich Research Park, Norwich NR4 7TJ, U.K.

S *Supporting Information*

ABSTRACT: Membrane proteins are key components of the plasma membrane and are responsible for control of chemical ionic gradients, metabolite and nutrient transfer, and signal transduction between the interior of cells and the external environment. Of the genes in the human genome, 30% code for membrane proteins (Krogh et al. *J. Mol. Biol.* **2001**, *305*, 567). Furthermore, many FDA-approved drugs target such proteins (Overington et al. *Nat. Rev. Drug Discovery* **2006**, *5*, 993). However, the structure−function relationships of these are notably sparse because of difficulties in their purification and handling outside of their membranous environment. Methods that permit the manipulation of membrane components while they are still in the membrane would find widespread application in separation, purification, and eventual structure−function determination of these species (Poo et al. *Nature* **1977**, *265*, 602). Here we show that asymmetrically patterned supported lipid bilayers in combination with AC electric fields can lead to efficient manipulation of charged components. We demonstrate the concentration and trapping of such components through the use of a "nested trap" and show that this method is capable of yielding an approximately 30-fold increase in the average protein concentration. Upon removal of the field, the material remains trapped for several hours as a result of topographically restricted diffusion. Our results indicate that this method can be used for concentrating and trapping charged membrane components while they are still within their membranous environment. We anticipate that our approach could find widespread application in the manipulation and study of membrane proteins.

The characterization of membrane proteins represents a significant challenge because of their instability outside of their membranous environment. Since most membrane proteins display a net charge on their extramembranous domains, they can be manipulated using an externally applied electric field. Previous studies have used DC fields to move charged phospholipids within a supported lipid bilayer environment[1] and shown that these fields in combination with mechanical scratching can be used to confine such species to small regions.[2−6] Furthermore, DC fields have been used to manipulate membrane-attached proteins through a combination of electrophoresis and electroosmosis.[7,8] Molecular ratchets, which are devices that use asymmetric potentials to move molecules against their concentration gradients, have been demonstrated in 3D geometries to move DNA molecules in solution.[9] Recently, patterned phase-separated bilayer systems[10] and microfluidic devices containing supported membranes[11] have been used to provide spatial control of membrane proteins. Here we present the first demonstration of a membrane trap that uses AC electric fields coupled with novel patterns to concentrate charged proteins within lipid bilayers. The patterns were designed to act like "fish traps", allowing facile ingress of charged components while impeding their egress. Nesting of such traps makes it possible to increase the trapping efficiency to allow a 30-fold increase in protein concentration. In comparison with previous work that has used DC fields in conjunction with mechanical scratching to create corrals of charged membrane components,[2,4,5] our method presents several advantages: First, charged species can be concentrated and trapped for a significant time as a result of slow diffusive recovery. Additionally, patterns can be nested within one another, providing a multiplicative concentration effect that has not been demonstrated previously. Furthermore, the use of AC fields allows electrodes to be placed closer together and hence to have smaller potentials. These advantages allow the method to be highly parallelized. The patterns presented here demonstrate only the concentration of charged species, but the separation of species according to their polarity or charge/size ratio would be possible using different geometries.

Lipid bilayers were formed within microcontact-printed fibronectin patterns following previously reported protocols.[12,13] The composition of the bilayers consisted of L-α-phosphatidylcholine (EggPC) with 0.2% Texas Red−1,2-dihexadecanoyl-*sn*-glycero-3-phosphoethanolamine (TR−DHPE), a fluorescently labeled lipid with a negative charge. The bilayers were rinsed with copious amounts of Milli-Q water prior to study. Lateral AC electric fields with a period of 2 h and amplitude of 62 V/cm were applied in the plane of the membrane in Milli-Q water, and the
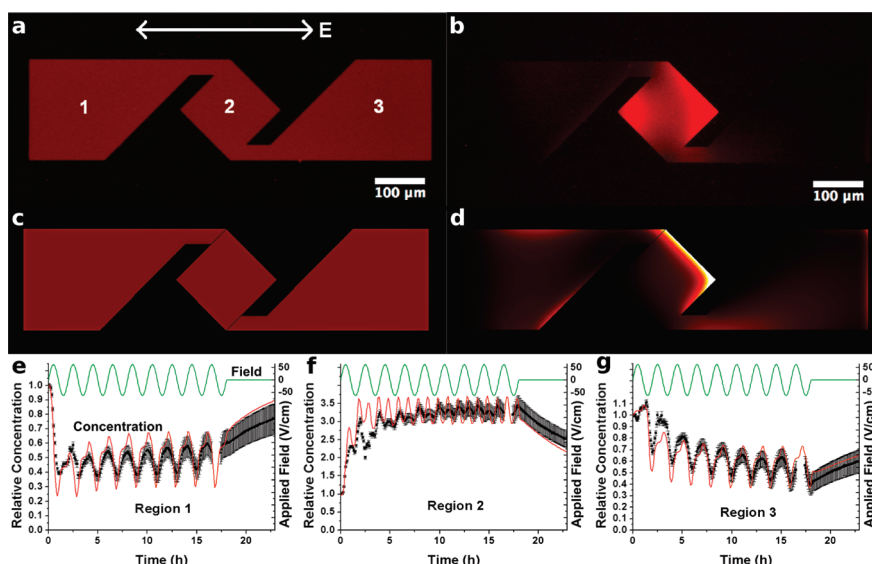
Figure 1. (a, b) Fluorescence micrographs of a TR−DHPE-containing lipid membrane (a) before and (b) after the application of an AC electric field **E** for nine cycles. (c, d) Results of FEA modeling of the membrane (c) before and (d) after are shown for comparison. (e−g) Plots of the relative average concentration (C/C_0) of charged lipid in regions marked 1−3, respectively. Red lines represent FEA data and black squares experimental data. Green lines represent the electric field due to the applied potential. The initial concentration C_0 of TR−DHPE was 0.2 mol %. After 18 h, the field was removed and the lipid allowed to egress by diffusion.

migration of charged species was monitored using epifluorescence microscopy. Details of the experimental methods are given in the Supporting Information(SI).

The simplest membrane trap comprised two reservoirs (Figure 1a, regions 1 and 3) and a central trap (Figure 1a, region 2). Charged species were driven into the central trap from the reservoir regions in alternate phases of the AC field cycle. Once within the central region, they could escape only via diffusion, leading to trapping of the mobile species. Diffusion coefficients were measured using fluorescence recovery after photobleaching (FRAP)[14,15] and found to be ∼1.5 μm^2/s for TR−DHPE in an EggPC supported lipid bilayer at 22 °C. At the start of each experiment, the distribution of TR−DHPE was uniform, as determined by fluorescence microscopy (Figure 1a). A sine-wave AC electric field was then applied, as shown in Figure 1. In the first half of each AC cycle, charged lipid (red) in reservoir 1 was driven into the central region, from which its egress was impeded. TR−DHPE in reservoir 3 was driven against the right-hand wall during this part of the cycle. In the second half of each cycle, TR−DHPE that had accumulated in region 2 remained there as a result of the protruding tooth on the opposite side, while TR−DHPE from reservoir 3 was also driven into this region. At a sufficiently low frequency, only one cycle was needed to achieve a nearly complete buildup of TR−DHPE in region 2. Upon removal of the field, the TR−DHPE remained localized because diffusion was impeded. Figure 1 shows fluorescence micrographs of the patterned lipid bilayer (a) before application of the electric field and (b) after application of an AC field for nine cycles. The concentration (C) of charged species within the lipid membrane was assumed to obey the Nernst−Planck equation,

$$\partial_t C(\mathbf{r},t) = \nabla \cdot [-D\nabla C(\mathbf{r},t) + ze\mu C(\mathbf{r},t)\nabla V(\mathbf{r},t)] \quad (1)$$

together with a modified Poisson equation,

$$\nabla \cdot [\varepsilon \nabla V(\mathbf{r},t)] = -\rho(\mathbf{r},t) = -fze N_A C(\mathbf{r},t) \quad (2)$$

where $V(\mathbf{r},t)$ is the applied potential; D and μ are the diffusivity and electrophoretic mobility of the ions, respectively; z is the valence; e is the elementary charge; ε is the electric permittivity; ρ is the charge density; and N_A is Avogadro's number. The values of μ and D are related via the Einstein relation $\mu = 0.6D/RT$, where R is the gas constant, T is the absolute temperature, and 0.6 is a factor accounting for the reduction in the effective mobility due to viscous drag from electro-osmosis.[1,2] We introduced the factor f into the Poisson equation to account for the unknown reduction of the effective charge density due to the presence of an electric double layer. Milli-Q water has a Debye screening length on the order of micrometers. In our calculations $z = -1$, $D = 1.5$ μm^2/s, and $T = 295$ K were used. Finite element analysis (FEA) software (COMSOL Ltd., Hatfield, U.K.) was used to model the membrane behavior and calculate the integrated charge in regions 1−3, as described in the SI.

Figure 1c,d shows the results of FEA modeling of the lipid behavior, while Figure 1e−g shows the normalized integrated charge obtained from both experiment and modeling for regions 1−3, respectively. The inclusion of electrostatic repulsion via the Poisson equation with an appropriate value of f led to good fits for the time dependence of the buildup of charged species. The modeling (red line) predicted a 3.5-fold increase in the concentration in the central region relative to the neighboring reservoirs, in agreement with the experimental data (black squares). Plots of the applied field are also shown for clarity (green lines). The best agreement with experiment was obtained for $f = 0.7$, which can be interpreted to indicate that either the electric double layer reduced the effective charge density in the bilayer by ∼30% (in Milli-Q water) or the mobility of the lipid layer was reduced. Interestingly, some of the TR−DHPE in the areas of highest concentration in region 2 displayed reduced mobility. Figure 1b shows that experimentally there was still a significant amount of charged lipid on the left-hand side of region 2, while the FEA calculation (Figure 1d) suggests that it should have all migrated to the right. This gives rise to discrepancies between theory and experiment at the extremities of each cycle. Cremer et al.[16] have shown that
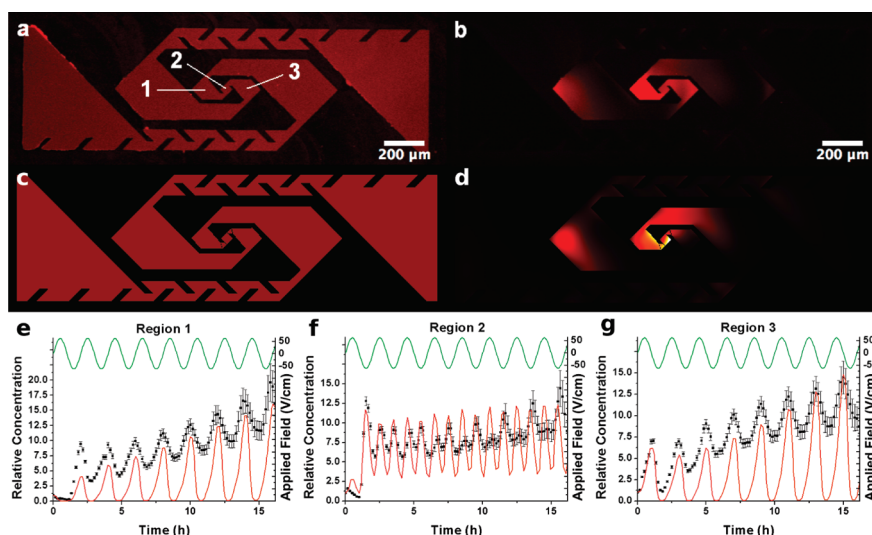
Figure 2. (a, b) Fluorescence micrographs of charged TR–DHPE in the patterned lipid membrane (a) before and (b) after the application of an AC field for eight cycles. (c, d) Corresponding FEA simulations for (c) before and (d) after. (e–g) Plots of the relative average concentration (C/C_0) of charged lipid for regions marked 1, 2, and 3, respectively. Black squares and red curves represent experimental data and FEA calculations, respectively. Green curves represent the applied field. The initial concentration C_0 of TR–DHPE was 0.2 mol %.

TR–DHPE has two conformations with slightly different mobilities, but this difference is too slight to account for the reduction in mobility observed here. It is possible that the reduction is related to depletion of EggPC lipids in the regions where the TR–DHPE concentration became very high. The localized reduction in mobility prevented any quantitative information regarding screening to be extracted from the f parameter. The field was removed at 18 h, allowing the TR–DHPE to relax back toward uniformity with an estimated half-life of 3.5 h (reducing the width of the channels allowing material to enter region 2 could be used to further increase the trapping time). It is noted that upon removal of the field, the theory best described the experiment when $f = 0$.

When the traps were nested, as shown in Figure 2, the simulations predicted a significant enhancement in concentration. Regions 1, 2, and 3 in Figure 2 were predicted to yield a 15-fold increase in concentration, while in the absence of charge repulsion, a 60-fold buildup was predicted for region 2. Figure 2 shows fluorescence micrographs of (a) the patterned lipid bilayer and (b) the bilayer after application of an AC field for eight cycles. The structure yielded an approximately 15-fold concentration increase toward the center, as expected. The best agreement between theory and experiment for region 2 was again found when $f = 0.7$. Interestingly, the best agreement for regions 1 and 3 was obtained when $f = 0.01$, which is significantly lower. This is possibly related to the reduced local mobility of the TR–DHPE in certain regions (see above). This reduced mobility was the primary reason that the experimental concentration for regions 1 and 3 did not vanish during each cycle, as predicted by the theory.

To demonstrate the manipulation of membrane proteins, a patterned bilayer was formed from proteoliposomes containing 0.25 wt % fluorescently labeled CymA, corresponding to ~146 proteins/μm² in each leaflet of the bilayer. CymA is a c-type tetraheme cytochrome with a molecular weight of 20 kDa that is membrane-bound by a putative membrane-spanning α-helix.[17] CymA is an ideal candidate for this system because it lacks large extra-membrane domains on both sides of the membrane. We previously showed that proteoliposomes with high protein

content do not readily rupture at a hydrophilic surface to form a bilayer but instead adsorb to the surface and remain intact.[18] Furthermore, many membrane proteins cannot be reconstituted above 1–2 wt %, hence adding to the importance of being able to manipulate and concentrate them once they are incorporated within the planar supported membrane. The protein was labeled with ATTO565, and the labeling was verified using gel electrophoresis (Supplementary Figure 1). There was at least one dye molecule present per protein. It was expected that upon bilayer formation, proteins would be presented in both orientations, such that extramembranous sections would be present at both the glass and ambient interfaces. Figure 3a,b shows fluorescence microscopy images at the early (cycle 1, 15 min) and late (cycle 8, 17 h) stages of field application. A video showing the accumulation of CymA during the application of the field is provided in the SI. By close examination of the fluorescence in the darker regions of the bilayer pattern, we were able to deduce that ~50% of the ATTO565-labeled CymA was immobile. This suggests that the CymA content was initially the same in each leaflet of the bilayer and that the CymA presented in the lower leaflet was immobile because of interactions with the substrate. This also demonstrates that our method can be used to separate proteins in the upper and lower leaflets from one another, which is potentially important for their study. Figure 3c–e shows the normalized average concentrations of regions 1, 2, and 3 respectively. An approximately 15-fold increase in intensity was seen in region 2, corresponding to a 30-fold increase in the protein concentration in the upper leaflet. This is equivalent to 4380 proteins/μm² in the upper leaflet. However, it was noted that in the apexes of the pattern, this concentration rose to ~11.3 wt %, corresponding to ~6600 proteins/μm² in the upper leaflet (~46-fold increase). The field was removed at 17 h, and the protein was allowed to diffuse. The half-life of the relaxation of protein in region 2 toward its initial state was estimated to be 2.2 h, demonstrating the trapping of the protein over relatively long periods of time.

In summary, we have demonstrated a novel method for concentrating and trapping charged membrane species within their membranous environments. Our results indicate that the CymA
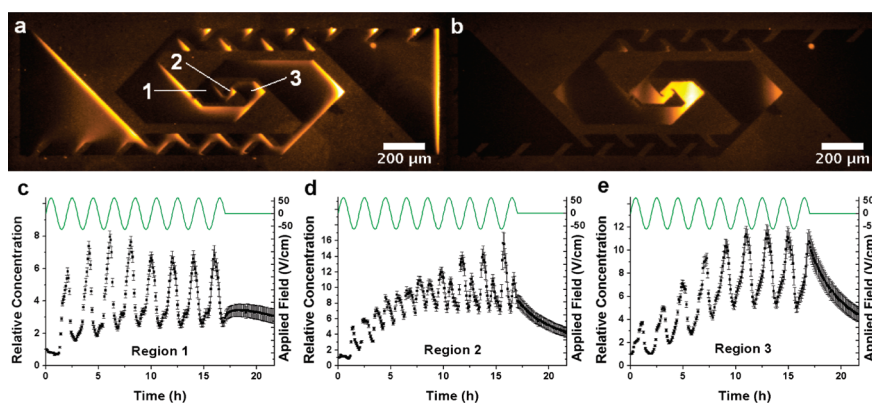
Figure 3. (a, b) Fluorescence micrographs of ATTO565-labeled CymA in the nested trap after application of a field for (a) 15 min and (b) 17 h. (c–e) Plots of the relative average concentration (C/C_0) (black squares) for regions 1, 2 and 3, respectively, showing a clear increase in protein concentration toward the center. Green lines show the applied field. The initial CymA concentration C_0 was ~0.25 wt %.

present in the lower leaflet was immobile. This implies that the final bilayer composition in the built-up region was highly asymmetric, with a 30-fold increase in concentration in the upper leaflet, and demonstrates that our approach can be used to separate components in different leaflets. The 30-fold increase corresponds to an average protein spacing of ~15 nm. In the apexes of the patterns, an even higher buildup was observed (46-fold increase), with the average protein spacing approaching 12.3 nm (cf. the diameter of a CymA protein, which is ~4 nm). We observed a 15-fold increase in charged lipid concentration and predict that a stronger applied field and partial charge screening via the use of buffer might allow a higher increase, with up to 60-fold predicted in the absence of charge repulsion. This could be further increased by optimization of the geometry. We observed a significant reduction in the mobility of charged species in the regions of highest density/confinement. In these regions, we might expect a major change in lipid composition through expulsion of the EggPC component and thus may have been seeing the effects of phase separation or local and reversible changes to the membrane structure. It is hoped that atomic force microscopy and high-resolution spectroscopy studies will further elucidate this phenomenon. Our approach is scalable and therefore allows pattern sizes to be reduced, which would permit higher-frequency AC fields to be used and a faster buildup to be achieved. However, smaller patterns would require greater field amplitudes to overcome diffusive effects and achieve tighter concentration profiles. This could be accomplished by placing the electrodes closer together. Furthermore, we anticipate that this method could be applied to native membranes, where it could be used to separate different components. In addition to "in-membrane" purification, protein crystallization is a possible future application.

ASSOCIATED CONTENT

S **Supporting Information.** Experimental procedures, SDS-PAGE analysis, a model of CymA, and a video clip (AVI). This material is available free of charge via the Internet at http://pubs.acs.org.

AUTHOR INFORMATION

Corresponding Author
s.d.evans@leeds.ac.uk

REFERENCES

(1) Stelzle, M.; Miehlich, R.; Sackmann, E. *Biophys. J.* **1992**, *63*, 1346.
(2) Groves, J. T.; Boxer, S. G. *Biophys. J.* **1995**, *69*, 1972.
(3) Groves, J. T.; Ulman, N.; Boxer, S. G. *Science* **1997**, *275*, 651.
(4) Groves, J. T.; Boxer, S. G.; McConnell, H. M. *Proc. Natl. Acad. Sci. U.S.A.* **1997**, *94*, 13390.
(5) Cremer, P. S.; Groves, J. T.; Kung, L. A.; Boxer, S. G. *Langmuir* **1999**, *15*, 3893.
(6) Van Oudenaarden, A.; Boxer, S. G. *Science* **1999**, *285*, 1046.
(7) Han, X.; Cheetham, M. R.; Sheikh, K.; Olmsted, P. D.; Bushby, R. J.; Evans, S. D. *Integr. Biol.* **2009**, *1*, 205.
(8) Yoshina-Ishii, C.; Boxer, S. G. *Langmuir* **2006**, *22*, 2384.
(9) Bader, J. S.; Hammond, R. W.; Henck, S. A.; Deem, M. W.; McDermott, G. A.; Bustillo, J. M.; Simpson, J. W.; Mulhern, G. T.; Rothberg, J. M. *Proc. Natl. Acad. Sci. U.S.A.* **1999**, *96*, 13165.
(10) Okazaki, T.; Tatsu, Y.; Morigaki, K. *Langmuir* **2010**, *26*, 4126.
(11) Jönsson, P.; Gunnarsson, A.; Höök, F. *Anal. Chem.* **2011**, *83*, 604.
(12) Bernard, A.; Renault, J. P.; Michel, B.; Bosshard, H. R.; Delamarche, E. *Adv. Mater.* **2000**, *12*, 1067.
(13) Kung, L. A.; Kam, L.; Hovis, J. S.; Boxer, S. G. *Langmuir* **2000**, *16*, 6773.
(14) Axelrod, D.; Koppel, D. E.; Schlessinger, J.; Elson, E.; Webb, W. W. *Biophys. J.* **1976**, *16*, 1055.
(15) Seiffert, S.; Oppermann, W. *J. Microsc.* **2005**, *220*, 20.
(16) Daniel, S.; Diaz, A. J.; Martinez, K. M.; Bench, B. J.; Albertorio, F.; Cremer, P. S. *J. Am. Chem. Soc.* **2007**, *129*, 8072.
(17) Field, S. J.; Dobbin, P. S.; Cheesman, M. R.; Watmough, N. J.; Thomson, A. J.; Richardson, D. J. *J. Biol. Chem.* **2000**, *275*, 8515.
(18) Dodd, C. E.; Johnson, B. R. G.; Jeuken, L. J. C.; Bugg, T. D. H.; Bushby, R. J.; Evans, S. D. *Biointerphases* **2008**, *3*, FA59.
(19) Laemmli, U. K. *Nature* **1970**, *227*, 680.
(20) Carter, K.; Gennis, R. B. *J. Biol. Chem.* **1985**, *260*, 10986.
(21) Rodrigues, M. L.; Oliveira, T. F.; Pereira, I. A. C.; Archer, M. *EMBO J.* **2006**, *25*, 5951.
(22) Arnold, K.; Bordoli, L.; Kopp, J.; Schwede, T. *Bioinformatics* **2006**, *22*, 195.